Sensors & Transducers, Vol. 182, Issue 11, November 2014, pp. 10-16

Sensors & Transducers

Analysis and Optimization of Composite to Steel Joints for Ships

*** Xiao-Wen Li, Ping Li, Zhuang Lin and Dong-Mei Yang**
College of Shipbuilding Engineering, Harbin Engineering University, Harbin 150001, China
* Tel.: 18945010506
* E-mail: heu119@sina.cn

Received: 2 June 2014 /Accepted: 29 August 2014 /Published: 30 November 2014

Abstract: Composite to steel joints as important components of ships are gradually found in the marine industry. The purpose of this study is to investigate mechanical performance and optimization methods of the composite sandwich to steel joints. The main emphasis was placed on the mechanical properties of a hybrid joint between a sandwich glass fibre reinforced plastic superstructure and a steel main hull. Based on the experiments of a base joint, a new finite element method was used to analyze a series of joints. The optimized joint was presented due to reducing weight and enhancing the mechanical performance. The strength of the optimized joint was evaluated by finite element method. The result is similar to the base joint and there is no high stress concentration in weak parts. The optimized joint has 40 % lower weight than the base joint, and the stress is only about 5 %~56 % of the base one. The results of the present work imply that the change of geometric parameters is an effective way to reduce weight and improve performance for the composite to steel joints.

Keywords: Composite, Joint, Mechanical properties, Ship.

1. Introduction

The connection of steel to composite is first used in aerospace industry, and begins expanding into other industries in the new century. The application of steel to composite joints has extended into the marine field as a novel method of incorporating lightweight composite superstructures to steel hulls. Owing to this hybrid joint, the ship can reduce the centre of gravity without weight increasing, and improving seakeeping ability and stability [1-5].

Hildebrand et al, [6] investigated solutions to joints between large FRP sandwich and steel structures. Based on the tests of static compression and bending, the static strength was found to be adequate compared to the traditional joints. Wright et al, [7] researched a fibre reinforced composite to steel connection for ship bulkheads. These joints were tested in tension, compression and lateral bending. They found that symmetric rather than asymmetric joints provide better strength characteristics. Clifford et al. [8] looked at very similar joints in lateral deflection. These specimens allowed investigation into the effect of joint geometry on structural performance, specifically the impact of the length of the steel insert on bending strength. By increasing the length of steel insert penetration into the core material, this failure move from core failure to yielding of the steel [9-12].

The static characterization of composite to steel joint, as the basic performance of the side structure, was investigated in this study. It is critical for the whole ability of a ship to stand large instantaneous loading [13]. In addition, numerical simulation of the

static behavior is undertaken incorporating experimental results. The optimized design was analyzed by finite element software Ansys.

2. Investigation of Composite to Steel Joint

2.1. Geometry

A traditional hybrid joint was adopted for the base design, which is illustrated in Fig. 1. The joint likes letter "y", so we call it y-joint for shot. This joint has a successful service experience as side structure in French La Fayette frigate [14]. It is composed of steel, balsawood core and GRP sandwich construction, has been subject to extensive studies in Euclid rtp3.21 project [15-18].

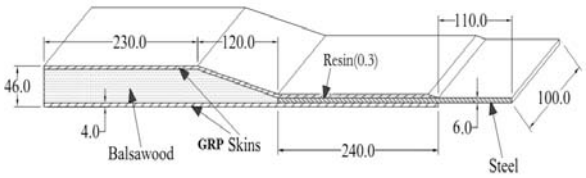

Fig. 1. Geometry of y-joint.

2.2. Materials

For y-joint, the steel insert is marine grade structural mild steel known as ST52, which has elevated yield strength. The reinforcement used in the GRP laminate is manufactured by Chomarat and described as an E-glass 3x1 twill, balanced woven roving [19]. This material has excellent drapeability. The adhesive in the reinforcement is vinylester resin, C411-45 manufactured by Dow Chemicals, which has resistance to moisture ingress [20]. And endgrain balsawood is used as core materials in the joint [21]. Material list is shown in Table 1.

Table 1. Material list.

Part		Material	Product code
Super-structure	Laminate	GRP	800S4(111A)
	Adhesive	Resin	C411-45
	Core	BalsaWood	AL600/10 CK-100
Main hull		Steel	ST52

2.3. Condition Design

The superstructure's length is smaller than half of the overall length, and it does not contribute to the global bending strength. So the y-joint as part of the superstructure just bear some vertical concentrated forces and its own weight when the ship in calm water. Finally, this paper mainly studied the static mechanical characterization of the y-joint under axial load.

3. Test

This test program was undertaken in the fortress test facility for axial tests. Fig. 2 [22] shows the test set up for the base design y-joint specimen. The static test was conducted in position control to observe any stress relief. The rate of loading for the static testing was 1 mm/min. Loads and displacements were obtained for the y-joint. The results are presented in Fig. 3 and Fig. 4 [22]. And Fig. 4 shows the test results. The load and displacement curve (L-D curve) presents linear at first. When the load is 65 kN, initial failure occurred in the border between steel and balsawood which corresponds to the maximum stress point in Fig. 4. And then, L-D curve keeps rising but presents nonlinear until the joint reach its ultimate bearing state. Corresponding to this ultimate state, the failure load and displacement of the y-joint is 108 kN and 4.3 mm. Fig. 3 shows the failure mode of the joint specimen. The joint generated peel debonding on the border of steel and lower laminate. And the shear failure occurred in taper area of the balsawood core. The upper laminate presents a little buckling at the position of x=-120 mm.

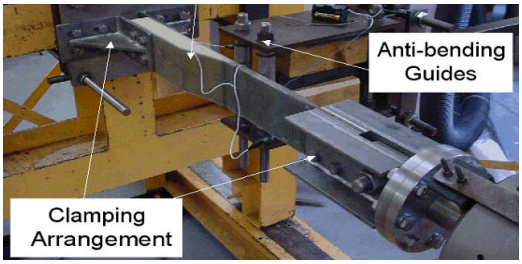

Fig. 2. Experimental test of the base joint specimen.

Fig. 3. Failure mode of the base joint.

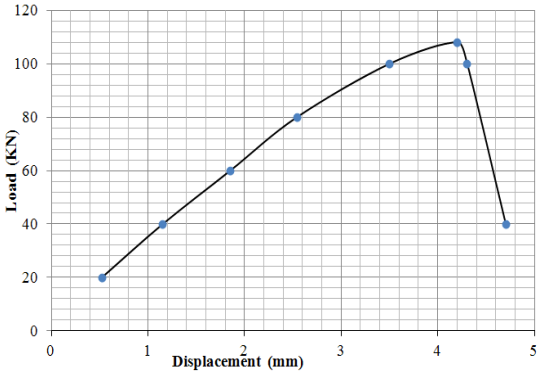

Fig. 4. Load and displacement curve of the base joint.

4. Finite Element Methods

4.1. FE Model

The commercial finite element software Ansys 13.0 is used to make a 2D plain strain model of the hybrid joint [23]. The element (Plane 82) used in the model is a plane 8 node isoparametric element with a 2X2 Gauss integration scheme [24]. It can be used for mixed automatic meshes. The finite element model and boundary condition are shown in Fig. 5 and Fig. 6, where the areas with different colors refer to different materials and the geometrical parameters are shown in Fig. 1. The elastic constants Ex, Ey, Gxy, vxy et cetera of each material in the local coordinate system are given in Table 2 together with the density of each part. The materials are assumed to be linear elastic, isotropic or orthotropic.

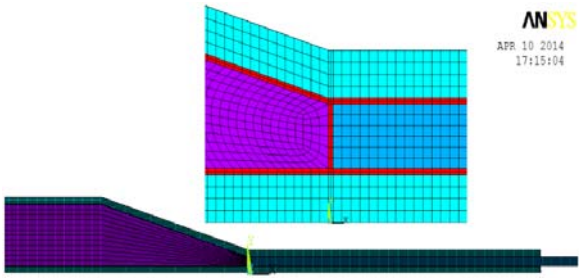

Fig. 5. FE model of the base joint.

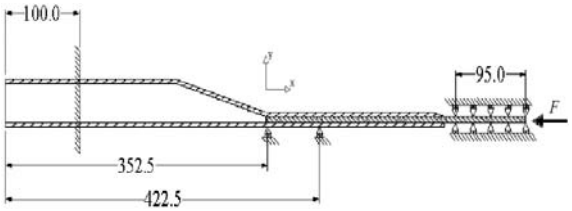

Fig. 6. Boundary conditions of the base joint.

Table 2. Material properties.

Property	GRP	Adhesive	Steel	Balsawood
E_x (MPa)	20600	2944.7	209000	56.951
E_y (MPa)	6700	2944.7	209000	2965
E_z (MPa)	20600	2944.7	209000	56.951
G_x (MPa)	3030	1323	80300	147
G_y (MPa)	3030	1323	80300	147
G_z (MPa)	3030	1323	80300	147
ν_{xy}	0.231	0.36	0.3	0.01
ν_{yz}	0.231	0.36	0.36	0.01
ν_{xz}	0.171	0.36	0.36	0.01
ρ (kg/m^3)	1680	1210	7833	180

4.2. FE Analysis

4.2.1. Analysis of Load Carrying Capacity

Fig. 7 shows both finite element and test results. The numerical simulation is satisfying, especially when the load is less than 65 kN where the maximal error of the model is less than 4 %. The ultimate bearing capacity of FE method is 102 kN, lower 5 % than the test result. And the displacement is 4 mm, 93 % of the test one. The stresses of critical parts in y-joint were calculated by finite element method, as shown in Fig. 8. Adhesive layer has stress concentration at the border between steel and balsawood where initial failure may occur easily. Balsawood core appears stress concentration, because this area has sudden geometrical change. There are two stress concentration points at x = 0 mm and x = -120 mm in the upper laminate of y-joint. Comparing Fig. 8 and Fig. 3, there are good correlation and same trend between simulation phenomena and experimental result. Conclusions as a result, the accuracy of the new method was further proved.

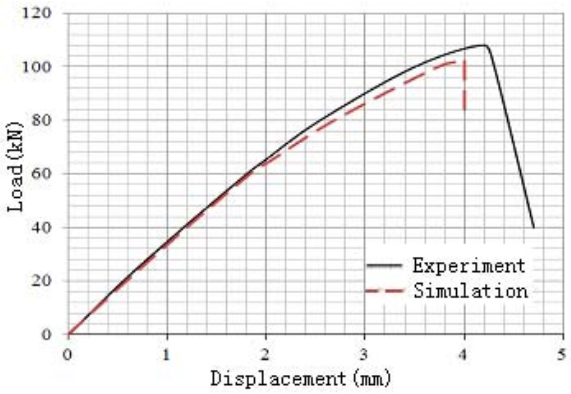

Fig. 7. FE result compared to experimental result for y-joint in compression.

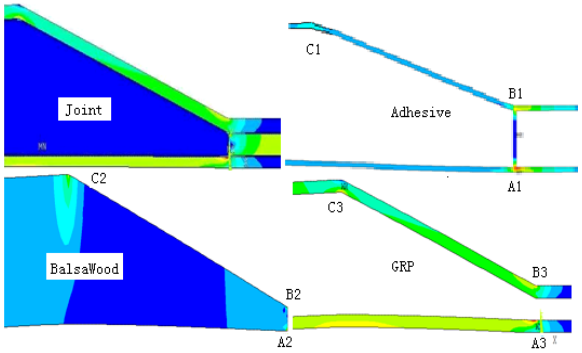

Fig. 8. Stress distribution of the base joint.

4.2.2. Stress Analysis

4.2.2.1. Adhesive Layer

Adhesive layer is the weak link in the whole joint, where occurs initial failure firstly. Fig. 9 illustrates the stress distribution of adhesive layer near the upper laminate. There are two obvious stress concentration at the position of x = 0 m and

x = -0.12 m, which corresponding to the point B1 and C1 in Fig. 8. The two stress concentrations are caused by the border of different materials (balsawood and steel) and geometry change. Fig. 10 shows the stress distribution of adhesive layer near the lower laminate. There is only one stress concentration at the border between balsawood and steel, which is consistent with the point A1 in Fig. 8. Fig. 11 depicts the stress distribution of adhesive layer between the balsawood and steel. Owing to the geometry and material change, the stress at the ends appears divergent.

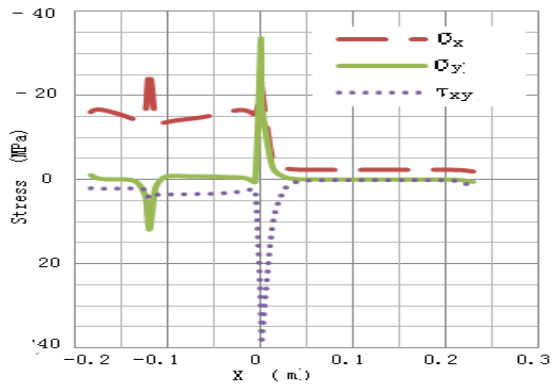

Fig. 9. Stress distribution in upper interface of adhesive Layer.

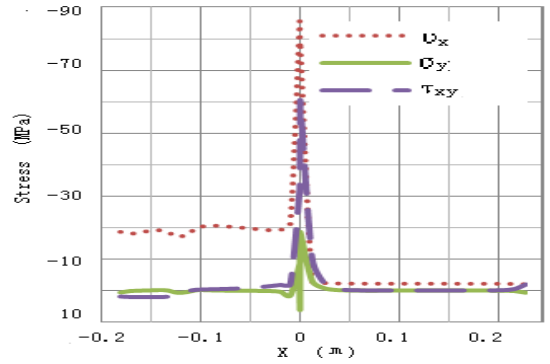

Fig. 10. Stress distribution in lower interface of adhesive Layer.

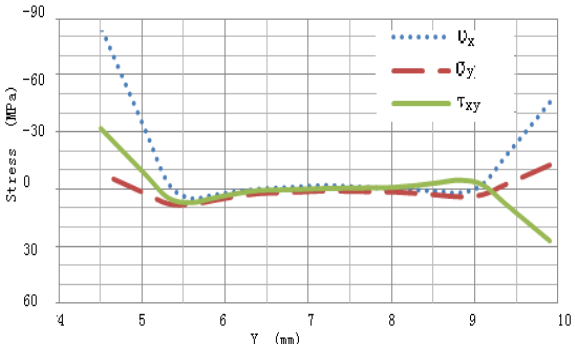

Fig. 11. Stress distribution of adhesive layer between the balsawood and steel.

4.2.2.2. Balsawood Stress

Fig. 12 shows the stress distribution of balsawood near the upper laminate. The stress presents a big fluctuation and there is an obvious stress change corresponding to point C2 in Fig. 8.

Fig. 13 explains that the shear stress plays a main role in the stress distribution of balsawood near the lower laminate, which matches the failure mode of balsawood in Fig. 3.

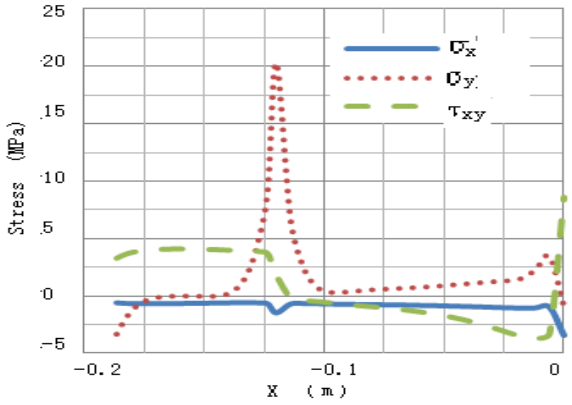

Fig. 12. Stress distribution in upper interface of balsawood core.

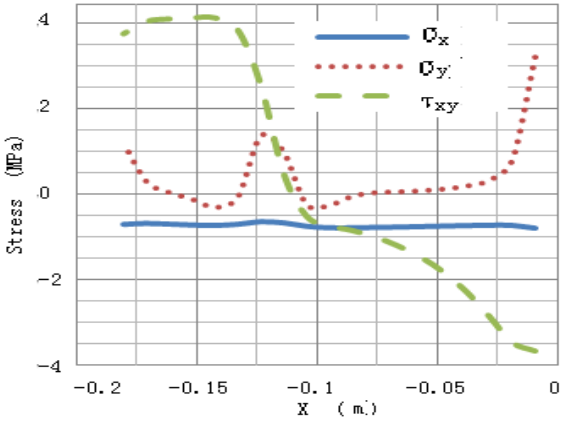

Fig. 13. Stress distribution in lower interface of balsawood core.

4.2.2.3. Laminate Stress

Fig. 14 and Fig. 15 show the main factor affecting the strength of laminate is σ_x, the direction of σ_x is consisting with the glass reinforcement fibre. The upper laminate has two stress concentrations at the positions of geometry change, which corresponds to the point of B3 and C3 in Fig. 8. The configuration of lower laminate is regular, and there is only one stress change at the position of x = 0, for the material change.

The other part's stress of the lower laminate distribute uniformly.

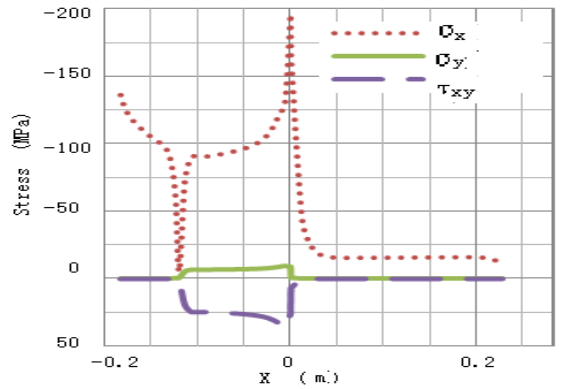

Fig. 14. Stress distribution in lower interface of top laminate.

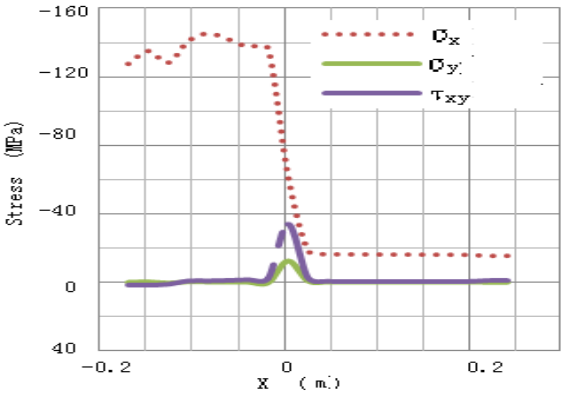

Fig. 15. Stress distribution in upper interface of top laminate.

All geometries are evaluated in the same manner, and finally the same criterion is used on the most promising configurations leading to final selection of the geometry for the optimized joint.

5. Optimization

The aim of optimization is to select lighter and stronger joint by detail design, instead of the big concept change. In order to save cost and time, this is done by Ansys program, as shown in Fig. 9.

5.1. Optimal Model

In this paper, the primary concern for designers is how to reduce ships' weight without compromising their performance. Such issues can usually be summarized as follows: minimize the structural weight with reliability constraints. The design model can be formulated as:

$$\text{Min} \qquad F(X) \le \sum \rho x_i l_i, \tag{1}$$

$$\text{Subject to} \qquad g_j(X) \le 0, \quad j = 1,2\cdots m \tag{2}$$

$$L_i \le x_i \le U_i, \quad i = 1,2\cdots n \tag{3}$$

where $X = \{x_1, x_2, \cdots, x_n\}$ is the design variable (as shown in Table 3) representing thickness of different parts, n is the number of the design variables. And $F(X)$ is the object function, ρ is the density, l_i is the length of different parts, $g_j(X)$ is the constraint conditions (as shown in Table 4) and m is the number of constrain conditions. L_i and U_i are the minimum and maximum limit of the i-th design variable.

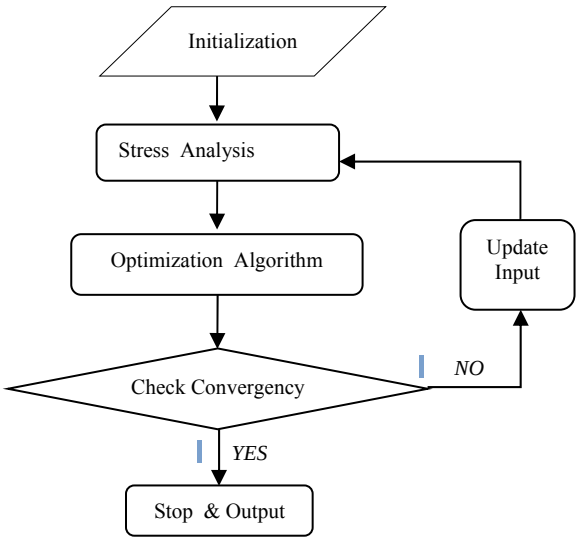

Fig. 9. Procedure of the optimum design.

Table 3. Design variables (mm).

Parameter name	Minimum value	Maximum value
GRP Thickness (TB)	2	10
Balsawood Thickness (TC)	20	90
Adhesive Thickness (TR)	0.2	1
Taper length (LT)	10	194
Overlap length (LO)	0	250

Table 4. Constrains of status variables.

Parameter name	X-direction Strength	Y-direction Strength	Shear Strength
GRP (MPa)	469	174	92.9
Balsawood (MPa)	4.36	19.4	12.9
Resin (MPa)	148	63.2	114
Displacement (mm)	0 ~ 3.5		

5.2. Optimization Method

The sub-problem approximation method can be described as an advanced zero-order method in that it requires only the values of the dependent variables, and not their derivatives. There are two concepts that

play a key role in the sub-problem approximation method: the use of approximations for the objective function and state variables, and the conversion of the constrained optimization problem to an unconstrained problem.

For this method, the program establishes the relationship between the objective function and the design variables by curve fitting. This is done by calculating the objective function for several sets of design variable values and performing a least squares fit between the data points. The resulting curve is called an approximation. Each optimization loop generates a new data point, and the objective function approximation is updated. It is this approximation that is minimized instead of the actual objective function.

5.3. Optimization Results

Fig. 10 and Fig. 11 illustrate the detail optimization procedure and iteration results. The optimal results are listed in Table 5.

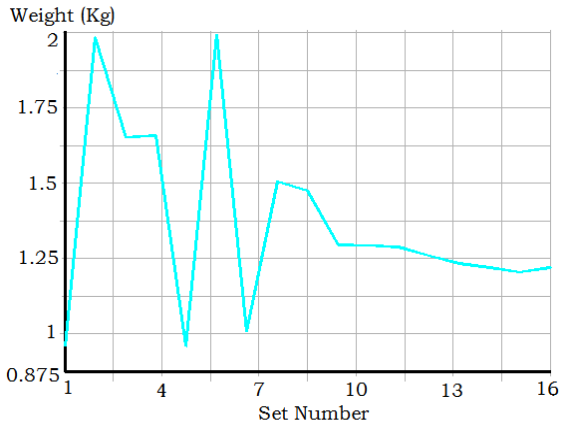

Fig. 10. Optimization procedure of y-joint's weight.

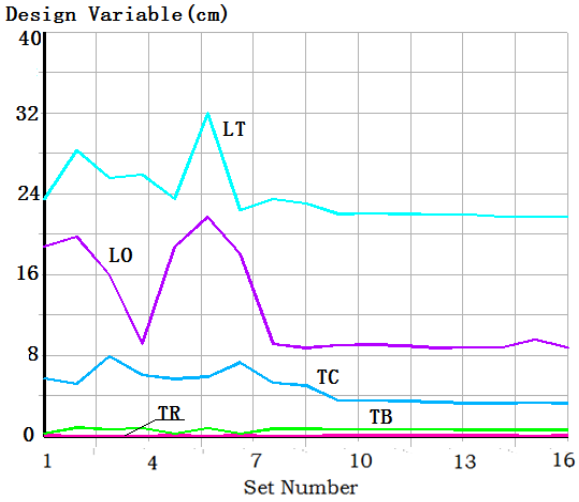

Fig. 11. Iteration results of the design variables.

Table 5. Optimal results.

Parameter name	Initial value	Optimal value
GRP Thickness (mm)	8.2	6.6
Balsawood Thickness (mm)	59	34
resin Thickness (mm)	0.58	0.64
Taper length (mm)	66	134
Overlap length (mm)	217	83
Weight (Kg)	2.454	1.467

The corresponding object value, namely the weight is 1.467 Kg. Comparing with the base joint, the optimal design has 40 % lower weight than the base one. Fig. 12 presents the stress level of the three different parts. The stress of the optimal joint was reduced in different degree, which is decreased by 5 % ~ 56 %.

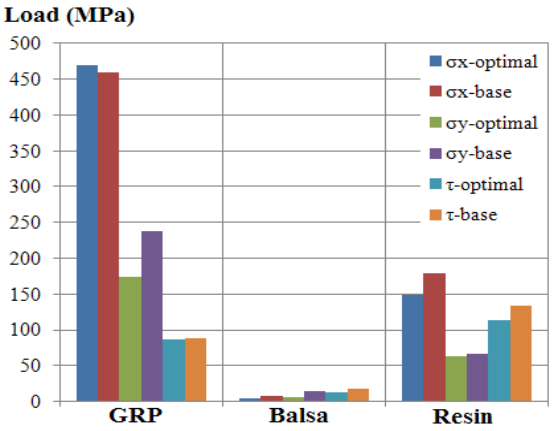

Fig. 12. Stress level of different parts.

6. Conclusions

Joints are the weakest parts of most structures, especially for the large ships with different materials. So the mechanical performance of the hybrid joint is critical to the whole ship. In this study, some properties of the composite to steel joint can be concluded.

a) For the y-joint, the main weakness lies in the border of steel and balsawood, where occurs high stress concentration, 14 % higher than other parts.

b) The performance of the y-joint can be improved by detail design instead of concept changes. The optimal design has 5 % ~ 56 % lower stresses than the base one by the optimization of geometric parameters, whose strength is much better.

c) Mechanical characterization and weight are both two important factors for the evaluation of joints. The optimized design's weight is 40 % of the base one and is good for larger ships.

This paper analyze the static mechanical characterization and optimization methods of composite to steel joint, especially load carrying capacity and stress character. and in the future study

will consider different sea conditions. It was proved that we can have better hybrid joints with lower weight and higher strength by some detail design instead of big concept change.

Acknowledgements

This project was supported by National Natural Science Foundation of China (Grant No 61004008), the Central Universities under Grant HEUCFR1001 and LBH-10138.

References

[1]. A. B. Hayman, et al, Use of composites in naval ships, in *Proceedings of the International Symposium Warship 2001 – Future Surface Warships*, London, Royal Institution of Naval Architects, 20–21 June 2001.

[2]. A. P. Mouritz, et al, Review of advanced composite structures for naval ships and submarines, *Composite Structures*, Vol. 53, Issue 1, 2001, pp. 21–41.

[3]. L. J. Hart-Smith, Design of adhesively bonded joints, F. L. Matthews, editor, Joining Fiber-reinforced Plastics, *Elsevier*, Barking, Essex, 1986, pp. 271–311.

[4]. K. Anyfantis, Adhesive bonding of dissimilar materials: Literature review. Technical report No. STL-279-F-09, *Shipbuilding Technology Laboratory, National Technical University of Athens*, 2009.

[5]. N. Konstantions, Analysis and design of composite to metal adhesively bonded joints, Doctor Thesis, *National Technical University of Athens*, 2012.

[6]. M. Hildebrand, Efficient solutions for joints between large FRP-sandwich and metal structures, in *Proceedings of the 19th SAMPE Europe International Conference*, Paris, France, 1998, pp. 417-428.

[7]. P. N. H. Wright, et al, Fibre reinforced composite-steel connections for transverse ship bulkheads, *Composites: Part A*, Vol. 29, Issue 10, 2000, pp. 549-557.

[9]. L. J. Hart-Smith, Adhesive bonding of composite structures – progress to date and some remaining challenges, *Journal of Composite Technology Research*, Vol. 24, Issue 3, 2002, pp. 133-153.

[9]. R. D. Adams, et al, Stress analysis and failure properties of carbon fibre reinforced plastic/steel double lap joints, *Journal of Adhesion*, Vol. 20, 1986, pp. 29-53.

[10]. R. D. Adams, Strength predictions for lap joints, especially with composite adherends, *Journal of Adhesion*, Vol. 30, 1989, pp. 219–242.

[11]. E. E. Theotokoglou, T. J. Moan, Experimental and numerical study of composite Tee-joints, *Journal of Composite Material*, Vol. 30, 1996, pp. 190-209.

[12]. R. D. Adams, J. A. Harris, The influence of local geometry on the strength of adhesive joints, *International Journal of Adhesion and Adhesives*, Vol. 7, Issue 2, 1987, pp. 69-80.

[13]. R. D. Adams, J. A. Harris, Strength prediction of bonded single lap joints by nonlinear finite element methods, *International Journal of Adhesion and Adhesives*, Issue 4, 1984, pp. 65-78.

[14]. A. Kapadia, Weight and cost comparison of base design structure to a given steel structure, Technical Report VT-2.3-C3-IP3.0, *EUCLID RTP 3.21,* 2002.

[15]. S. M. Clifford, C. I. C. Manger, T. W. Clynet, Characterization of a glass-fibre reinforced vinylester to steel joint for use between a naval GRP superstructure and a steel hull, in *Proceedings of the International Conference on Composite Structures (ICCS)*, Melbourne, Australia, 19 November 2001, Vol. 57, No. 1-4, pp. 59-66.

[16]. R. D. S. G. Campilho, et al, Strength prediction of single and double lap joints by standard and extended finite element modeling, *International Journal of Adhesion and Adhesives*, Vol. 31, Issue 5, 2011, pp. 363-372.

[17]. J. Cao, L. Grenesdt, Test of a redesigned glass-fiber reinforced vinylester to steel joint for use between a naval GRP superstructure and a steel hull, *Composite Structures*, Vol. 60, 2003, pp. 439-445.

[18]. J. Cao, L. Grenesdt, Design and testing of joints for composite sandwich/steel hybrid ship hulls, *Composites: Part A*, Vol. 35, 2004, pp. 1091–1105.

[19]. Helmuth Toftegaard, Aage Lystrup, Design and test of lightweight sandwich T-joint for naval ships, *Composites: Part A*, Vol. 36, 2005, pp. 1055–1065.

[20]. C. S. Smith, P. Murphy, Response of hybrid GRP/steel superstructures to blast loading theory and experiment, Advances in Marine Structures-2, *Elsevier Applied Science*, London, 1991, pp. 392-415.

[21]. R. A. Shenoi, F. L. M. Violette, A Study of Structural Composite Tee Joints in Small Boats, *J. Compos. Mater,* 1990, Vol. 24, No. 6, pp. 644-666.

[22]. Stephen William Boyd, Strength and durability of steel to composite joints for marine application, Doctor thesis, *University of Southampton*, 2006.

[23]. G. Cavallini, et al, Boundary element modeling and analysis of adhesive bonded structural joints. *Electronic Journal of Boundary Elements*, Issue 4, 2006, pp. 31-48.

[24]. A. Andrianakis, Experimental and numerical study of a steel-to-composite adhesive joint under bending moments, Diploma Thesis, *School of Naval Architecture and Marine Engineering, National Technical University of Athens*, 2011. (in Greek).